

# Remnants of greenstone sequence from the Archaean rocks of Rajasthan

Rajani Upadhyaya, B. L. Sharma Jr\*, B. L. Sharma Sr and A. B. Roy

Department of Geology, M. L. Sukhadia University, Udaipur 313 001, India

\*Present address: Department of Geology, North-Eastern Hill University, Kohima 797 001, India

---

An interesting association of granitoid-amphibolite-metasediments occurs around Jagat, southeast of Udaipur in Rajasthan. Lying a little south of the area from where 3.3-billion-year-old gneisses have been reported, these rocks compare well with the known greenstone associations of Archaean age. The mafic and granitoid rocks show chemical affinity with the modern volcanic arc rocks.

---

THE geological map of southeastern Rajasthan prepared by Heron<sup>1</sup> shows a number of metasedimentary-metavolcanic units separated by outcrops of gneiss-granite rocks, the latter described as Banded Gneissic Complex (BGC). The stratigraphic position of BGC in relation to the metasedimentary metavolcanic units belonging to the Aravalli system, Delhi system and the Raialo series<sup>1</sup> has been debated over the last four decades or so<sup>2,3</sup>. Recently available isotopic dates<sup>4,5</sup>, however, confirm that the gneiss-granite rocks mapped as the BGC over a large area, are truly Archaean in age, and have undergone extensive ductile deformation and reconstitution during the Proterozoic<sup>3</sup>. The 3.3-billion-year-old gneisses, the oldest known so far from this part of the Indian shield, occur near Jhamarkotra, southeast of Udaipur. Detailed mapping by us in the area a little south of Jhamarkotra revealed an association of gneiss-

granite-amphibolite-metasedimentary rocks which compares well with the well-known granite-greenstone belts around the world. Here we report field and chemical characteristics of these rocks. This might help in understanding the early crustal evolution in the region. A reference may be made in this connection to the report of Sargur-type banded iron formation by Sahoo and Mathur<sup>6</sup> from the neighbourhood of the study area around Jagat (Figure 1) about 30 km southeast of Udaipur.

## Lithology and field relationship

Lithologically, the rocks of the Jagat area can be divided into three main groups, namely the granitoids, the amphibolites (including poorly metamorphosed dolerite) and the metasediments. The granitoids cover by far the largest area, followed by the amphibolites. The metasedimentary units, which include carbonates, calc-silicate rocks, quartzite, iron formations and pelitic schists, on the other hand, occur as small bands and irregular enclaves within the granitoid rocks.

The granitoids are of three different types: pink granites, leucogranites and grey gneisses. The last one seems to be the most common of the three. The pink granite, because of its colour and composition, can be



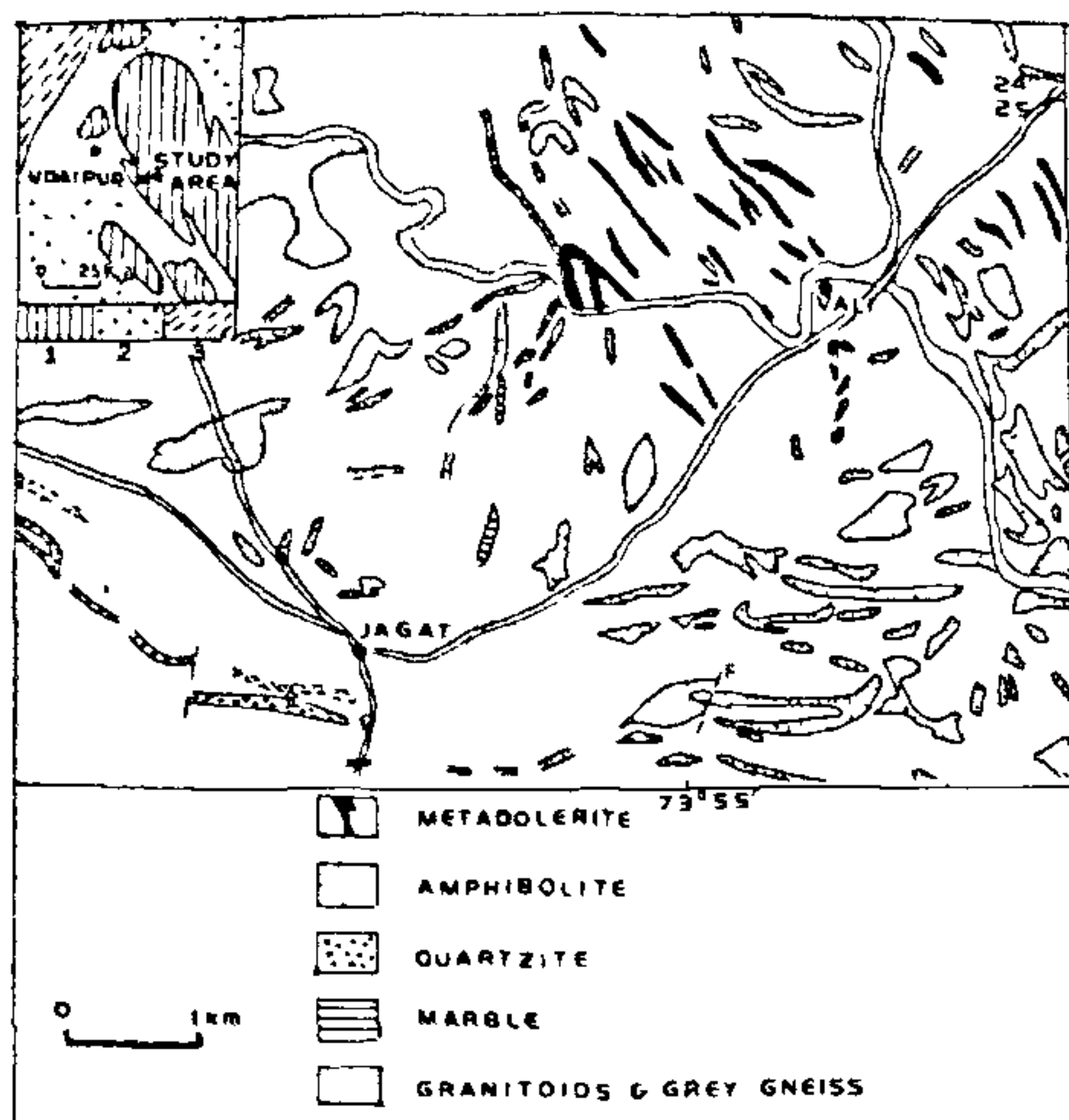


Figure 1. Geological map of the Jagat area, southeast of Udaipur, Rajasthan. Inset, location map of the area: 1, BGC (Mewar Gneiss); 2, Aravalli Supergroup; 3, Delhi Supergroup.

easily identified as the youngest intrusive bodies cross-cutting almost all the lithological units except the youngest mafic intrusives. The leucogranitoids are massive and occur in close association with grey foliated gneisses. The contact between the two units is always gradational. Thus in outcrops one can see foliated grey gneisses passing gradually into massive leucogranite, and only locally showing faint traces of foliation. If the nature and folding of gneissic foliation is studied carefully, it would appear that the grey gneiss itself constitutes a number of genetic types. Structural evidence suggesting presence of more than one phase of grey gneiss is illustrated by the presence of enclaves of grey-gneisses showing complexly folded foliation in the midst of gneisses showing planar foliation.

Like the granitoids, the amphibolites can also be classified into three types: small, irregular-shaped outcrops within the grey gneisses; larger, relatively linear bodies of amphibolites cofolded with gneisses (locally cross-cutting gneissic and type 1 amphibolite foliation); and youngest dykes intruding all the rock components of the area.

In the geological map prepared for the Jagat area, the outcrop pattern formed by the Type 2 amphibolites (Figure 1) presents a picture of extremely ductile

Table 1. Mean and standard deviation of major and trace element contents of granitoids of the Jagat area

|  | Pink granites<br>(cluster M <sub>1</sub> ) |         | Leucogranites<br>(cluster M <sub>2</sub> ) |         | Grey gneisses<br>(cluster M <sub>3</sub> )<br>(cluster M <sub>4</sub> ) |         |               |         |
|--|--|---------|--|---------|---|---------|---------------|---------|
|  | Mean<br>(n=21)                             | SD      | Mean<br>(n=10)                             | SD      | Mean<br>(n=15)  | SD      | Mean<br>(n=9) | SD      |
| Major elements (wt%)   |  |         |  |         |   |         |               |         |
| SiO <sub>2</sub>   | 73.22                                      | 1.74    | 74.88                                      | 0.836   | 68.43   | 2.31    | 63.00         | 2.95    |
| TiO <sub>2</sub>   | 0.167                                      | 0.112   | 0.21                                       | 0.138   | 0.379   | 0.151   | 0.56          | 0.318   |
| Al <sub>2</sub> O <sub>3</sub>   | 14.79                                      | 0.863   | 14.63                                      | 0.656   | 16.31   | 0.899   | 17.44         | 2.89    |
| Fe <sub>2</sub> O <sub>3</sub>   | 0.569                                      | 0.467   | 0.394                                      | 0.301   | 1.36  | 0.894   | 2.28          | 1.78    |
| FeO  | 0.443                                      | 0.313   | 0.456                                      | 0.412   | 1.61  | 0.674   | 3.18          | 2.04    |
| MnO  | 0.014                                      | 0.008   | 0.013                                      | 0.011   | 0.037   | 0.012   | 0.065         | 0.042   |
| MgO  | 0.368                                      | 0.333   | 0.372                                      | 0.326   | 1.11  | 1.01    | 2.08          | 1.89    |
| CaO  | 1.026                                      | 0.447   | 1.23                                       | 0.724   | 2.88  | 0.893   | 3.01          | 2.01    |
| Na <sub>2</sub> O  | 3.93                                       | 0.613   | 5.51                                       | 0.996   | 4.91  | 0.868   | 3.98          | 1.20    |
| K <sub>2</sub> O   | 4.02                                       | 1.067   | 0.839                                      | 0.414   | 1.55  | 0.771   | 2.11          | 1.45    |
| P <sub>2</sub> O <sub>5</sub>  | 0.123                                      | 0.241   | 0.176                                      | 0.280   | 0.29  | 0.272   | 0.231         | 0.164   |
| Mol. Al <sub>2</sub> O <sub>3</sub> /<br>Na <sub>2</sub> O + K <sub>2</sub> O +<br>CaO | 1.17                                       | —       | 1.20                                       | —       | 1.098   | —       | 1.086         | —       |
| K <sub>2</sub> O/Na <sub>2</sub> O   | 1.09                                       | —       | 0.167                                      | —       | 0.324   | —       | 0.96          | —       |
| Trace elements (ppm)   |  |         |  |         |   |         |               |         |
| Li   | 4.19                                       | 3.19    | 5.3  | 4.52    | 12.2  | 6.10    | 29.11         | 25.55   |
| Rb   | 85.28                                      | 27.13   | 28.4                                       | 12.23   | 50.53   | 20.21   | 98.33         | 57.60   |
| Sr   | 200.33                                     | 87.63   | 187.7                                      | 120.75  | 401.4   | 148.61  | 415.33        | 275.70  |
| Ba   | 1645.80                                    | 1260.86 | 597.7                                      | 1063.57 | 1742.66   | 1960.11 | 1518.56       | 1678.96 |
| Cr   | 26.19                                      | 10.7    | 23.5                                       | 9.83    | 40.53   | 15.80   | 42.78         | 37.49   |
| Cu   | 3.93                                       | 13.14   | 20.7                                       | 14.69   | 17.4  | 7.84    | 26.0          | 23.42   |
| Ni   | 22.43                                      | 8.99    | 23.00                                      | 11.18   | 36.66   | 6.58    | 47.56         | 17.60   |
| Zn   | 17.48                                      | 39.70   | 10.00                                      | 10.35   | 31.23   | 20.33   | 71.44         | 65.52   |
| K/Rb   | 412.50                                     | —       | 250.00                                     | —       | 278.67  | —       | 258.75        | —       |
| Ca/Sr  | 29.05                                      | —       | 42.00                                      | —       | 54.66   | —       | 55.56         | —       |
| Rb/Sr  | 0.586                                      | —       | 0.267                                      | —       | 0.196   | —       | 0.282         | —       |

polyphase deformation. The grade of metamorphism during these deformation phases ranged between middle and upper amphibolite facies. The last phase of deformation is manifested by a series of low-dipping shear zones formed under lower amphibolite to greenschist facies metamorphism.

On the basis of field data, the following stratigraphic model has been erected for the Jagat area:

Dolerite dykes (Type 3 amphibolites)

Pink granites

Shearing and low *P-T* metamorphism

Leucogranitoids

*Polyphase folding and amphibolite facies metamorphism*

Emplacement of Type 2 amphibolites and metasediments (?) Grey gneisses with small enclaves of amphibolites (komatiitic) and metasediments.

### Petrochemistry and tectonic setting of rocks

#### Granitoids

The average chemical analysis of the different granitoids is given in Table 1. Statistically, the granitoids group into four clusters, which correspond to pink granites (cluster  $M_1$ ), leucogranitoid (cluster  $M_2$ ) and grey gneisses (clusters  $M_3$  and  $M_4$ ) respectively. As the normative Ab-An-Or diagram (Figure 2) shows, the compositions of leucogranitoids and the grey gneisses range in the field of tonalite trondhjemite-granodiorite (TTG). The pink granites mostly fall in the field of true granites and their average major element composition matches well with the average of the granite-adamelite.

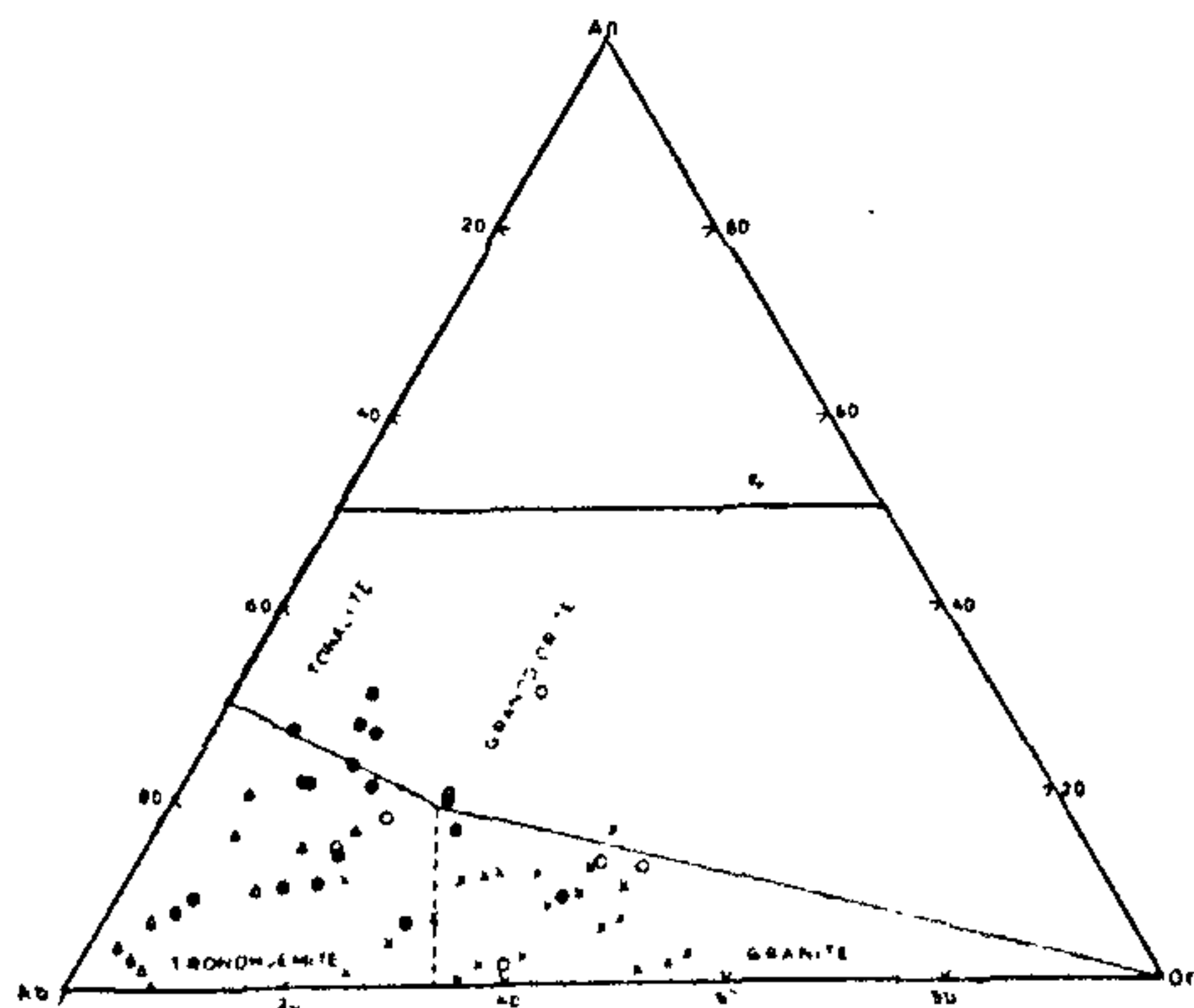


Figure 2. Normative An-Ab-Or diagram (after O'Connor<sup>15</sup>). Closed circles and open circles, two clusters of grey gneisses; open triangles leucogranites; crosses, pink granite.

There is a degree of uniqueness in the composition of the leucogranitoids (cluster  $M_2$  rocks) in having higher values of  $SiO_2$  and lower values of  $Al_2O_3$  compared to those of grey gneisses (clusters  $M_3$  and  $M_4$ ). The leucogranitoids, therefore, can rightly be described as the high silica low alumina granite of Barker<sup>7</sup>.

Compatibility of the Jagat granitoids with those of the Archaean is brought out clearly in the  $(La/Yb)_N$  vs  $Yb_N$  diagram<sup>8</sup> (Figure 3). In the AFM diagram (Figure 4) all the components of the Jagat granitoids together

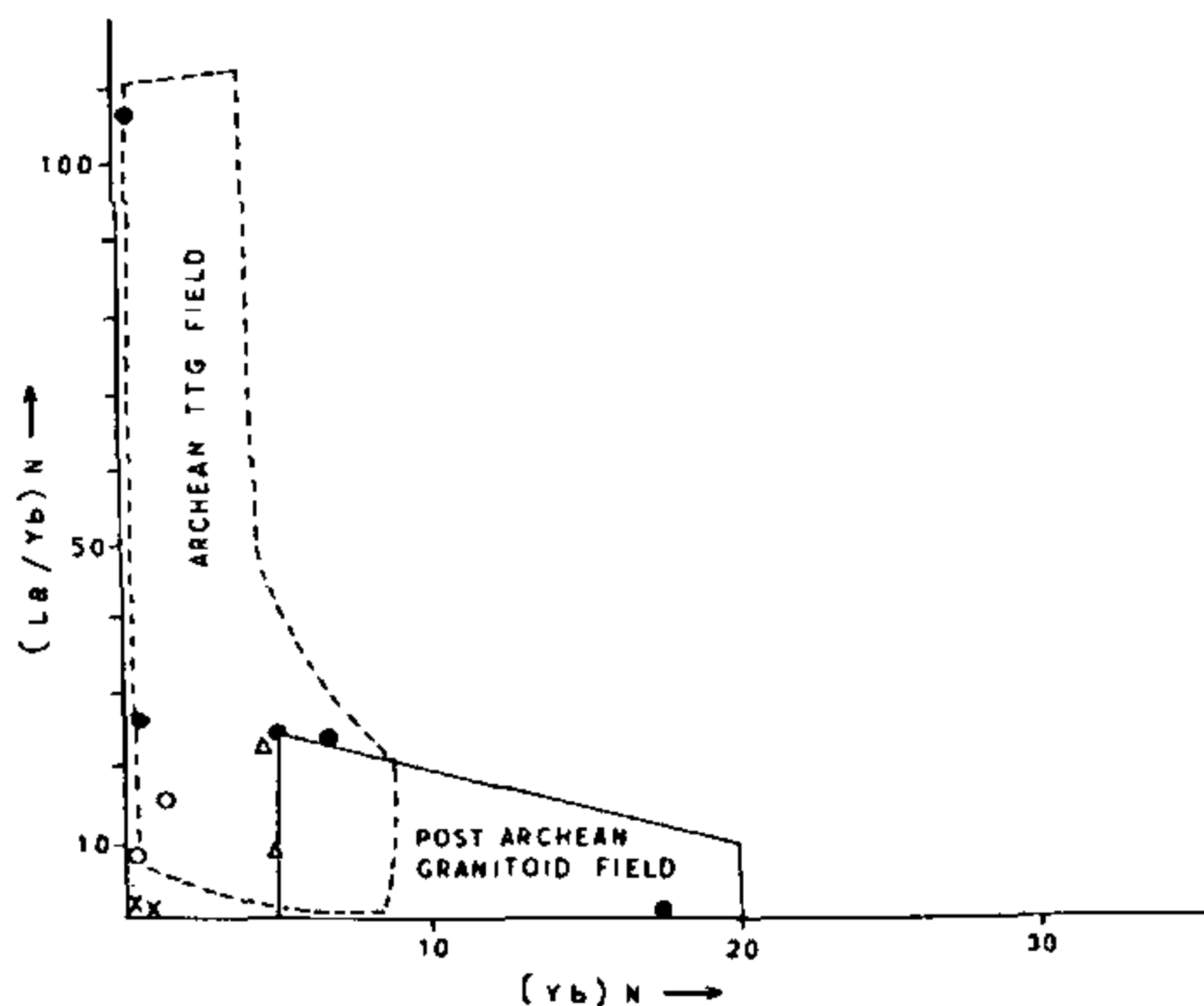


Figure 3.  $(La/Yb)_N$  vs  $(Yb)_N$  plot showing fields of Archaean and post-Archaean granitoid rocks. Most of the Jagat granitoids fall in the Archaean field. Symbols as in Figure 2.

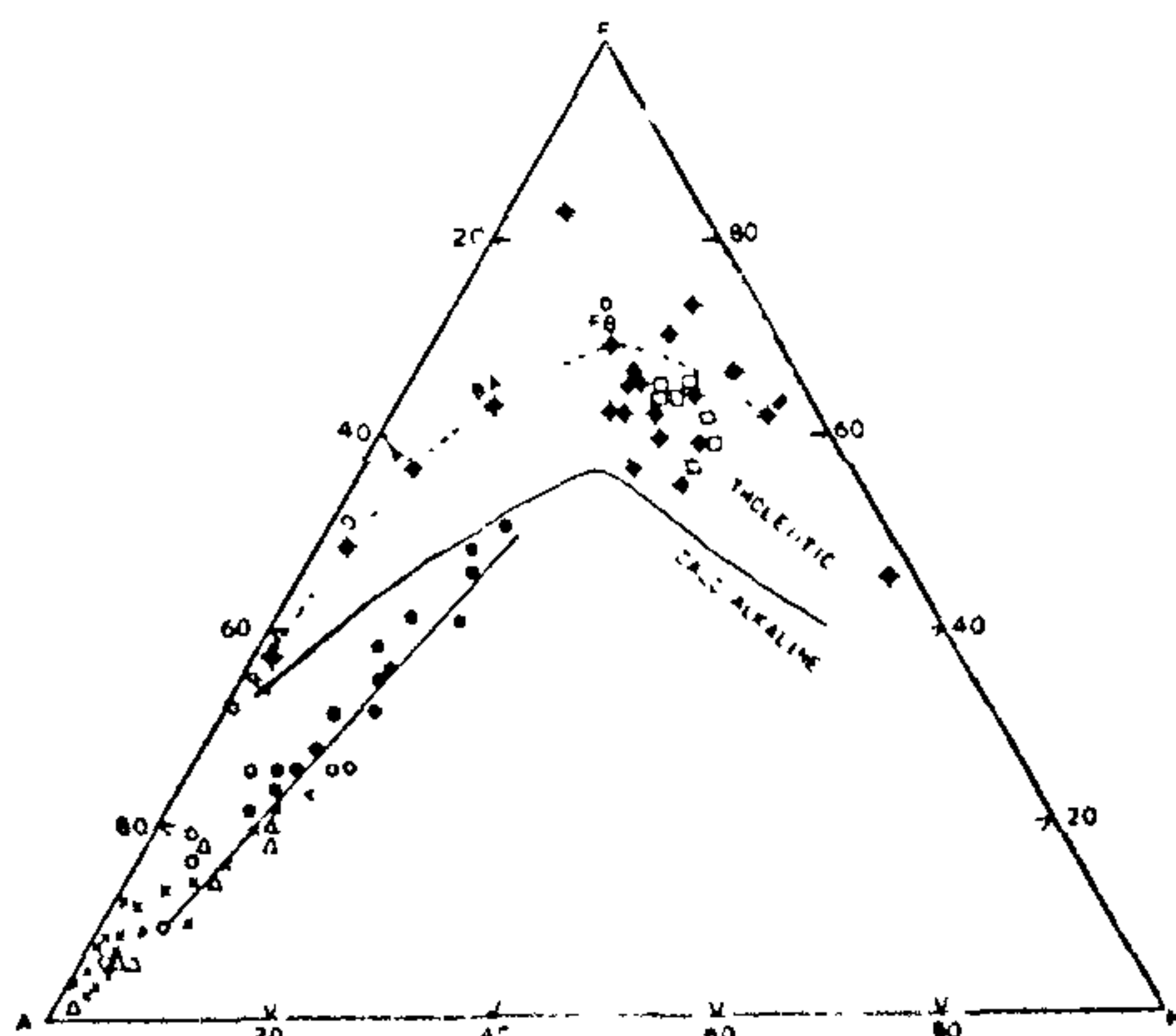


Figure 4. Plots of Jagat granitoids and amphibolites in AFM diagram. Closed and open circles, two clusters of grey gneisses, open triangles, leucogranite; crosses, pink granite. The discontinuous line represents the tholeiitic differentiation series, basalt (B), ferro-basalt (FB), basaltic andesite (BA), andesite (A), dacite (D) and rhyolite (R). Closed circles with plus sign, Type 2 amphibolites, open squares, Type 3 amphibolites.

show a linear trend in the calcalkaline field. The other chemical parameters such as Rb vs (Y + Nb) and Nb vs Y plots<sup>9</sup> (Figure 5) also suggest similarity of the granitoids with those occurring in the Cenozoic volcanic arc (Figure 5).

*Mafic rocks*

Some of the mafic rocks of the Jagat area, which occur as small, irregular-shaped enclaves within the grey gneisses (Type 1 amphibolites), are komatiitic in chemistry, showing high values of MgO, Cr and Ni (Table 2, analysis no. 1). It must, however, be noted that these rocks occur rather rarely compared to tholeiitic metabasalts grouped under Type 2 and Type 3 amphibolites. The Type 2 amphibolites which are cofolded with the grey gneisses and younger metabasaltic dykes (Type 3 amphibolites) are comparable in their chemical analysis, showing only minor differences in the average values TiO<sub>2</sub>, Al<sub>2</sub>O<sub>3</sub>, Fe<sub>2</sub>O<sub>3</sub>, SiO<sub>2</sub> and Ba,

Cr, Cu and Ni (cf. Table 2, analyses nos. 2 and 3). Plots in the AFM diagram (Figure 4) reveal the tholeiitic composition of these mafic rocks. Both types of amphibolites are quartz and hyperstene normative and a few of these have normative olivine.

Diagrams of Pearce<sup>10</sup> were used to define the possible tectonomagmatic setting of the Jagat amphibolites. The rocks plot in the CAB/LKT field in the F<sub>1</sub>-F<sub>2</sub> diagram and in the LKT field in the F<sub>2</sub>-F<sub>3</sub> diagram (Figure 6). In Mullen's<sup>11</sup> (MnO) × 10-TiO<sub>2</sub>-(P<sub>2</sub>O<sub>5</sub>) × 10 diagram (Figure 7) most of these amphibolites plot in

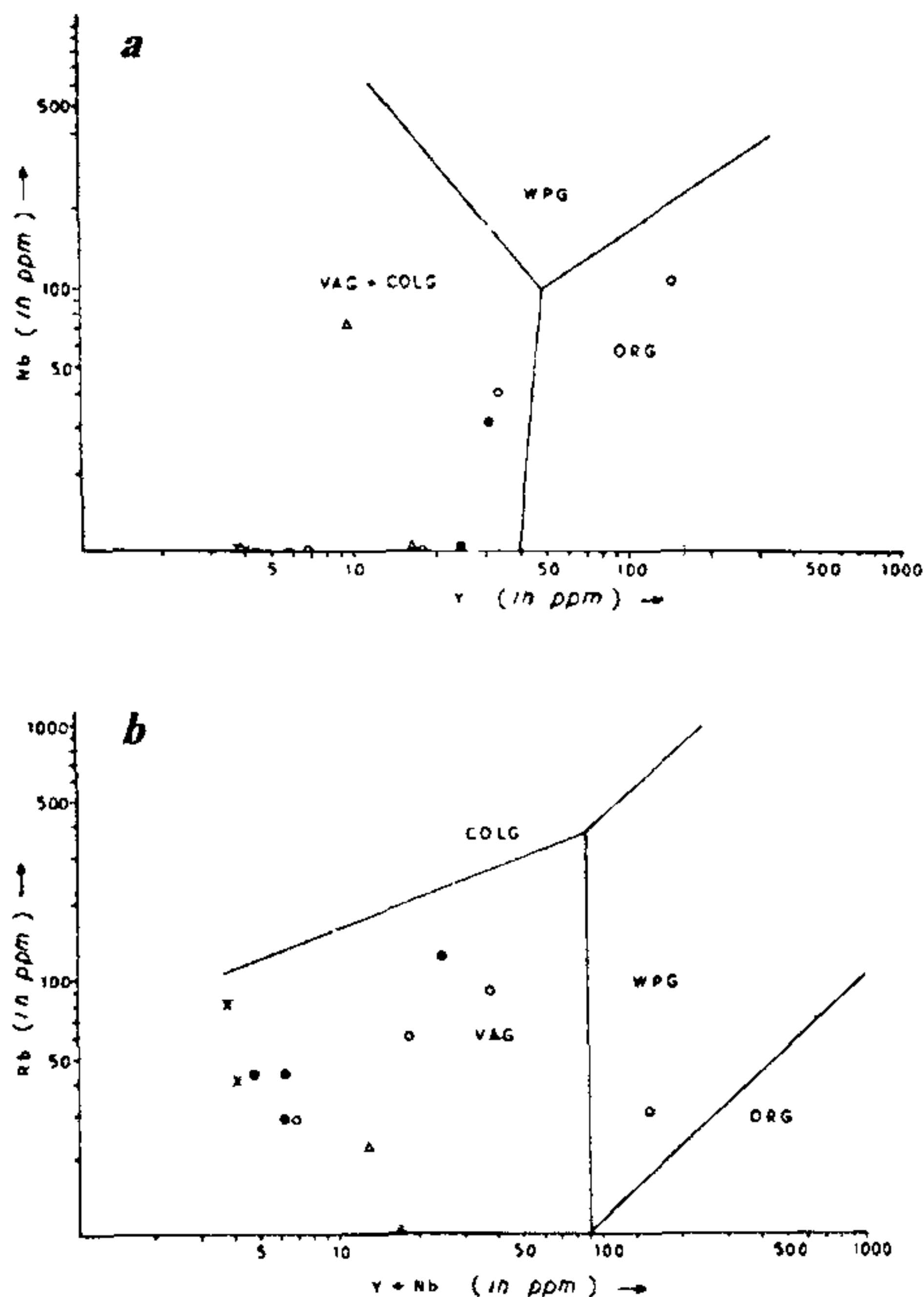


Figure 5. Nb vs Y and Rb vs (Y + Nb) diagrams showing the fields of low potassium tholentites (LKT), ocean floor basalts (OFB), calc-alkaline basalts (CAB), shoshonites (SHO) and within plate basalts (WPB). Closed circles, Type 2 amphibolites, open squares, Type 3 amphibolites

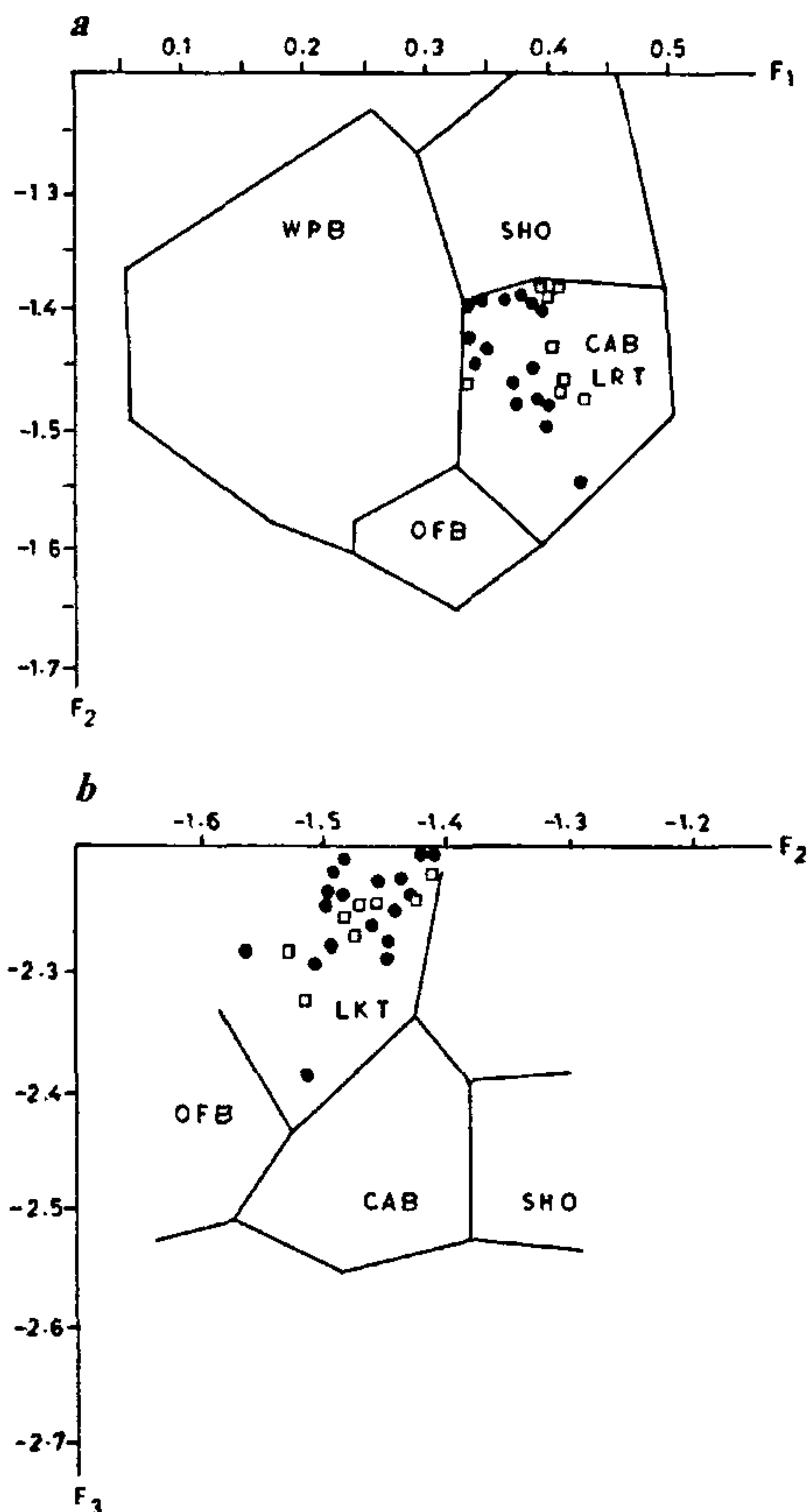
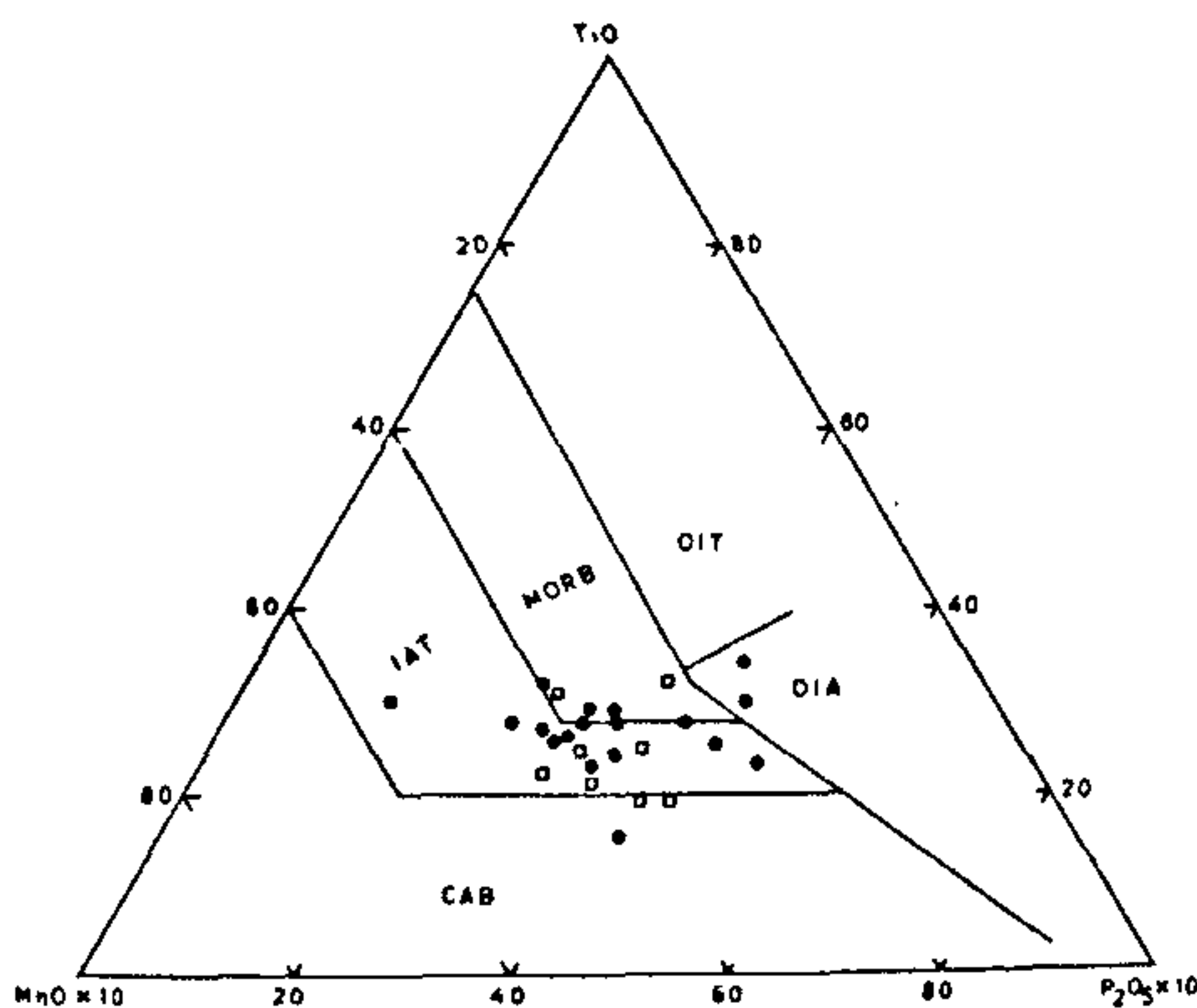


Figure 6. Plots of discriminant functions F<sub>1</sub>-F<sub>2</sub> (a) and F<sub>2</sub>-F<sub>3</sub> (b) showing the fields of low potassium tholentites (LKT), ocean floor basalts (OFB), calc-alkaline basalts (CAB), shoshonites (SHO) and within plate basalts (WPB). Closed circles, Type 2 amphibolites, open squares, Type 3 amphibolites



**Table 2.** Major and trace element composition of mafic rocks and iron ore formations

| Sl. no.                                | 1               | Type 2     | Type 3    | 4                | 5               |
|--|-----------------|------------|-----------|------------------|-----------------|
| Sample no.                             | 6K <sub>8</sub> | (n=17) av. | (n=8) av. | 10D <sub>2</sub> | 3M <sub>4</sub> |
| Oxides (wt %)                          |                 |            |           |                  |                 |
| SiO <sub>2</sub>                       | 52.28           | 50.4       | 49.32     | 52.32            | 32.37           |
| TiO <sub>2</sub>                       | 0.87            | 1.93       | 1.54      | 0.49             | 9.00            |
| Al <sub>2</sub> O <sub>3</sub>         | 7.76            | 13.51      | 14.71     | 3.69             | 7.68            |
| Fe <sub>2</sub> O <sub>3</sub>         | 0.99            | 4.33       | 3.89      | 1.76             | 12.49           |
| FeO                                    | 11.92           | 10.78      | 10.86     | 31.12            | 12.96           |
| MnO                                    | 0.23            | 0.23       | 0.23      | 0.55             | 0.32            |
| MgO                                    | 14.89           | 5.5        | 6.0       | 2.25             | 1.19            |
| CaO                                    | 8.35            | 8.59       | 8.95      | 2.89             | 8.65            |
| Na <sub>2</sub> O                      | 0.51            | 2.22       | 2.13      | 1.26             | 1.67            |
| K <sub>2</sub> O                       | 0.16            | 0.75       | 0.71      | 1.33             | 2.06            |
| P <sub>2</sub> O <sub>5</sub>          | 0.23            | 0.26       | 0.24      | 0.27             | 0.11            |
| Total                                  | 98.19           |            |           | 98.23            | 98.5            |
| Mg No.                                 | 67.66           | 40.12      | 42.76     | 12.09            | 8.19            |
| FeO <sub>v</sub> /MgO                  | 1.86            | 2.82       | 2.45      | 12.82            | 20.34           |
| CaO/Al <sub>2</sub> O <sub>3</sub>     | 1.08            | 0.66       | 0.61      | 0.78             | 0.49            |
| CaO/Na <sub>2</sub> O+K <sub>2</sub> O | 12.46           | 2.01       | 3.24      | 1.12             | 2.32            |
| K <sub>2</sub> O/Na <sub>2</sub> O     | 0.31            | 0.34       | 0.32      | —                | 1.23            |
| S.I.                                   | 51.38           | 23.35      | 24.9      | 6.71             | 3.92            |
| Trace elements (ppm)                   |                 |            |           |                  |                 |
| Li                                     | 17              | 19         | 19.63     | 5                | 21              |
| Rb                                     | 17              | 19.43      | 24.89     | 8                | 70              |
| Sr                                     | 42              | 157.53     | 166.84    | 13               | 426             |
| Ba                                     | 101             | 546.6      | 426       | 135              | 618             |
| Cr                                     | 1371            | 89.18      | 144.93    | 62               | 166             |
| Cu                                     | 13              | 89.18      | 175.85    | 11               | 27              |
| Ni                                     | 891             | 116.59     | 148.15    | 74               | 63              |
| Zn                                     | 154             | 156.94     | —         | 41               | 188             |
| Cr/Ni                                  | 1.54            | 0.67       | 0.75      | 2.84             | 2.02            |
| Rb/Sr                                  | 0.4             | 0.201      | 0.203     | 0.62             | 0.16            |
| K/Rb                                   | 70              | 476.9      | 206.6     | 1380             | 240             |



**Figure 7.** Mullen's<sup>12</sup> triangular diagram showing plots of Jagat amphibolites in the field of island arc tholeiite (IAT) and mid-oceanic ridge basalt (MORB). Symbols as in Figure 6.

the field of island arc tholeiites (IAT) and mid-oceanic ridge basalt (MORB).

Very little information is now available on the chemistry of the metasedimentary units which include a

few bodies of quartzite (bearing fuchsite mica), mica schists, marble and iron-stone formations. The latter units contain both banded magnetite (ilmenite) quartzite (BMQ) and quartz-grunerite rocks (with or without garnet). The occurrence of BMQ is relatively rare compared to the quartz-grunerite rocks. The chemical compositions of the latter rocks are given in Table 2 (4 and 5). Rocks such as these are quite common in the greenstone belts of Karnataka<sup>12</sup>.

## Conclusions

Isotopic data from the neighbouring area suggest three important thermal events<sup>5</sup>, corresponding to the emplacement of TTG gneisses of Jhamarkotra at 3.3 billion years ago (Ga), emplacement of Maoli-Rakhwal amphibolite at 2.83 Ga, and metamorphic reconstitution of minerals at 2.45 Ga. If these dates are taken as representative of the Archaean events in this part of the Indian shield, then the total period of granitoid-greenstone evolutionary history must have spanned a period of about one billion years. This long interval is quite compatible with that of the other granitoid-greenstone terranes of the world<sup>13,14</sup>.

Though the association of the rocks occurring around Jagat looks very similar to that of the South

Indian greenstone belts, the available data from Rajasthan point out some glaring contrasts, some of which are: (i) paucity of ultramafic rocks; (ii) total absence of conglomerate and coarse clastic rocks; and (iii) no known metal mineralization of Archaean age, except for some localised occurrences of barite deposits.

These differences may be critical to the recognition of greenstone belt evolutionary process<sup>12</sup> in this part of the Indian shield. At the present state of our knowledge it is difficult to reconstruct the geometry and areal extent of the greenstone belts. What we see today are the extensive dismembered patches of greenstone rocks amidst the sea of granitoid rocks.

1. Heron, A. M. *Mem. Geol. Surv. India*, 1953, **79**, 1.
2. Naha, K., Chaudhuri, A. K. and Mukherji, P., *Contrib. Mineral. Petrol.*, 1967, **15**, 191.
3. Naha, K. and Roy, A. B., *Precambrian Res.*, 1983, **19**, 217.
4. Choudhary, A. L., Gopalan, K. and Sastry, C. A., *Tectonophysics*, 1984, **10**, 131.
5. Gopalan, K., Macdougall, J. D., Roy, A. B. and Murali, A. B., *Precambrian Res.*, 1990, **48**, 287.
6. Sahoo, K. C. and Mathur, A. K., *J. Geol. Soc. India*, 1991, **38**, 299.
7. Barker, F., in *Trondhjemites, Dacites and Related Rocks* (ed. Barker, F.), Elsevier, Amsterdam, 1979, pp. 1-12.
8. Martin, H., *Geology*, 1986, **14**, 753.
9. Pearce, J. A., Harris, N. B. W. and Tindle, A. G., *J. Petrol.*, 1984, **25**, 956.
10. Pearce, J. A., *J. Petrol.*, 1976, **17**, 15.
11. Mullen, E. D., *Earth Planet Sci. Lett.*, 1983, **62**, 53.
12. Janardhan, A. S., Swamy, N. S. and Capdevilla, R. J., *Geol. Soc. India*, 1986, **28**, 179.
13. Groves, D. I. and Batt, W. E., in *Archaean Geochemistry* (eds. Kroner, A., Hanson, G. N. and Goodwin, A. M.), Springer, Berlin, 1986, pp. 73-98.
14. Pichamuthu, C. S. and Srinivasan, R., in *Precambrian of South India* (eds. Naqvi, S. M. and Rogers, J. J.), Geological Society of India, Bangalore (Memoir 4), 1983, pp. 121-139.
15. O'Connor, J. K., *US Geol. Surv. Prof. Paper*, 1965, 525-B, 79-84.

ACKNOWLEDGEMENTS. We thank the University Grants Commission for financial assistance for the study, and Dr N. K. Chauhan, Dr D. K. Nagori and Dr Harsh Bhu for their help.

Received 26 December 1991; revised accepted 26 May 1992